Electron Energy Dependence of Regioselective Chloride Ion Loss from Polychlorodibenzo-*p*-dioxins. Relationship between Resonance Electron Energies and Virtual Orbital Energies

V. D. Berkout, P. Mazurkiewicz, and M. L. Deinzer*

Contribution from the Department of Chemistry and Environmental Health Sciences Center, Oregon State University, Corvallis, Oregon 97331-7301

Received May 11, 1998

Abstract: Regiospecifically chlorine-37-labeled polychlorodibenzo-*p*-dioxins (PCDDs) undergo electron energy-dependent regioselective chloride ion loss when analyzed by electron capture negative ion mass spectrometry using an electron monochromator to supply the slow monoenergetic electrons. Three negative ion resonances, produced with electrons of energies <0.5, ∼1, and ∼4 eV are associated with the production of chloride ions from PCDDs. Negative ion resonances for the production of molecular ions of higher PCDDs were recorded with electrons of energies <0.2 eV. Dichlorodibenzo-*p*-dioxins and some trichlordibenzo-*p*-dioxins showed no molecular ions. A correlation was found between the experimental electron attachment energies and the virtual orbital energies calculated by modified density functional theory methods using the B3LYP/D95// B3LYP/D95 level of theory. The results from these correlations strongly suggest that all negative ion-forming processes for this class of compounds are initiated from π^* states. The loss of chloride ion from transient negative PCDD ions requires $\pi^*-\sigma^*$ orbital mixing.

Introduction

Electrons interact with electrophilic molecules to produce negative ions in many chemical processes. Yet, compared to positive ions, relatively little is known about the mechanisms of gas-phase negative ion formation, partly because they involve resonance processes with low-energy electrons that are difficult to generate and control. In the standard procedure electrons boiled from the filament are cooled by collisions with a reagent gas in the ion source.[1] This method produces not only thermalized electrons with large energy spreads but also positive ions that can react with neutral molecules to give unpredictable amounts of adventitious product ions whose spectra are difficult to interpret.[2,3] Wide variations in electron energies in different instruments my also be a factor responsible for poor reproducibility of negative ion spectra from different laboratories.[4]

Devices to produce low-energy electrons (0−50 eV) with nearly monoenergetic (0.005−0.1 eV) distributions have actually been known for at least three decades.[5,6] The construction of these devices, called electron monochromators (EM) was prompted by early interests in determining accurate ionization potentials and energy states of atoms and molecules for which the 1−2 eV energy spreads of the electrons available from hot filaments were unacceptable. Prototype electron monochromator−mass spectrometer (EM−MS) instruments were also con-

structed early on,[7] but it was not until relatively recently that several groups, using in-house constructed instruments, have begun to study electron−molecule interactions in greater detail.[8−12]

In the EM−MS instrument monoenergetic electrons are produced by crossed electric and magnetic fields, which eliminates the need for the reagent gas in the ion source.[13] The energies of the electrons can be tuned to match the negative ion resonances of the ions of interest. This feature of the electron monochromator allows a more detailed investigation of the mechanisms of negative ion formation and also provides a method to produce another dimension of analytical information for identifying molecules.[12] Polychlordibenzo-*p*-dioxins (**I**) are
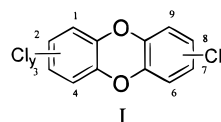
ideal compounds for studying the relationships between resonance energies and their electronic structures. The availability

(1) Dougherty, R. C. *Anal. Chem.* **1981**, *53,* 625A−636A.

(2) Stökl, D.; Budzikiewicz, H. *Org. Mass Spectrom.* **1982**, *17,* 376−381.

(3) Stökl, D.; Budzikiewicz, H. *Org. Mass Spectrom.* **1982**, *17,* 470−474.

(4) Arbogast, B.; Budde, W. L.; Deinzer, M.; Dougherty, R. C.; Eichelberger, J.; Foltz, R. D.; Grimm, C. C.; Hites, R. A.; Sakashita, C.; Stemmler, E. *Org. Mass Spectrom.* **1990**, *25,* 191−196.

(5) Marmet, P.; Kerwin, L. *Can. J. Phys.* **1960**, *38,* 787−796.

(6) Simpson, J. A. *Rev. Sci. Instrum.* **1964**, *35,* 1699−1704.

(7) Fox, R. E.,; Hickam, W. M.; Grove, D. J.; Kjeldaas, T., Jr. *Rev. Sci. Instrum.* **1955**, *26,* 1101−1107.

(8) Christophorou, L. G.; McCorkle, D. L.; Christodoulides, A. A. Electron Attachment Processes. In *Electron-Molecule Interactions and Their Applications;* Christophorou, L. G., Ed.; Academic Press Inc.: Orlando, FL, 1984; Vol. 1, pp 477−617.

(9) Oster, T.; Kühn, A.; Illenberger, E. *Int. J. Mass Spectrom. Ion Processes* **1989**, *89,* 1−72.

(10) Ingólfsson, O.; Weik, F.; Illenberger, E. *Int. J. Mass Spectrom. Ion Processes* **1996**, *155,* 1−68.

(11) Burrow, P. D.; Gallup, G. A.; Fabrikant, I. I.; Jordan, K. D. *Aust. J. Phys.* **1996**, *49,* 403−423.

(12) Laramée, J. A.; Mazurkiewicz, P. H.; Berkout, V.; Deinzer, M. L. *Mass Spectrom. Rev.* **1996**, *15,* 15−42.

(13) Laramée, J. A.; Kocher, C. A.; Deinzer, M. L. *Anal. Chem.* **1992**, *64,* 2316−2322.

of pure regiospecifically enriched chlorine-37 polychloro-dibenzo-*p*-dioxin isomers[14] provided a unique opportunity to investigate the regiochemical dependence of reductive dechlorination on electron energies. Questions concerning possible chlorine isotope effects could also be addressed. Finally, certain PCDD isomers are reported to be highly toxic,[15] and the techniques adapted here may have important practical utility, since recent efforts to implement methods for analyzing trace levels of these compounds depend on the use of electron capture negative ion mass spectrometry (ECNI-MS),[16] a technique that may be more sensitive than electron impact ionization for these molecules.

Experimental Section

Negative Ion Mass Spectrometry. Electron energy-dependent regioselective loss of chloride ions and analysis of negative ion resonances (NIRs) were performed on an HP 5982A dodecapole mass spectrometer retrofitted with an electron monochromator (EM–MS) that creates a well-defined and narrow beam (± 0.1 eV) of tunable electrons over an energy range of 0–15 eV.[13] Calibration of electron energies was achieved by using the well-known NIRs for hexafluorobenzene ($M^{-\cdot}$, $\epsilon_{max} = 0.03$; $C_6F_5^{-\cdot}$, $\epsilon_{max} = 4.5$ and 8.3 eV)[17] as references. Calibration was performed immediately before and after data acquisition. The ion source temperature was 140–160 °C unless otherwise stated. The PCDDs were introduced into the instrument by splitless injection on an HP 5710A gas chromatograph equipped with a DB-5 10m × 0.25 mm i.d. capillary column with 0.25-μm film thickness. The $[^{35}Cl^-]/[^{37}Cl^-]$ ion abundance ratios were recorded at specified electron energies. The reliability of the chlorine isotope ratio measurements was checked against the natural abundance ratio of chlorine isotopes produced from CH_2Cl_2 in the EM–MS instrument. Comparative data for chloride ion loss from PCDDs were acquired under ECNI-MS conditions using methane reagent gas on double focusing JEOL DX-300 and Kratos MS-50 mass spectrometers.

Chemicals. Regiospecific chlorine-37 enriched dichloro-, trichloro-, tetrachloro-, pentachloro-, and hexachlorodibenzo-*p*-dioxins were synthesized in-house.[14] Nonlabeled dioxins were purchased from AccuStandard.

Determination of Chlorine-37 Isotope Enrichment. Isotope enrichments were measured on Kratos MS50, JEOL DX-300, and Finnigan 4023 instruments under ECNI-MS conditions by recording the isotope patterns of the molecular ion signals. Isotopic enrichments of regiospecifically ^{37}Cl-labeled PCDDs were determined by an algorithm that seeks to minimize the χ^2 between a synthetically generated isotopic pattern based on a modified binomial expansion and the experimental data.[18] The synthetic isotope pattern is generated from the equation $(x + y)^m(A + B)$, where x and y are natural abundances of ^{35}Cl and ^{37}Cl, respectively, and m is the number of natural chlorines present. A and B are the ^{35}Cl and ^{37}Cl enrichment residuals due to the enrichment. Enrichments for labeled dioxins ranged from 74 to 96 atom %.[14]

Determination of Regioselective Chloride Ion Loss. The relative chloride ion loss was determined as described previously.[18] Briefly, chloride ion loss from the positions is determined from the observed $[^{35}Cl]/[^{37}Cl]$ ratios by solving the simultaneous equations

$$ax + cy = I_A$$

$$bx + dy = I_B$$

where I_A is the relative intensity of the ^{35}Cl$^-$ ion and I_B is the relative intensity of the ^{37}Cl$^-$ ion obtained from the mass spectrum. The

coefficient c is the residual of ^{35}Cl, and d is the relative excess of ^{37}Cl from regiospecific labeling. The value x is the fraction of chlorine lost from the unenriched position(s), and y is the fraction of chlorine loss from the position enriched with ^{37}Cl. Natural abundances of the chlorine isotopes ^{35}Cl and ^{37}Cl were determined by mass spectrometry to be 0.7555 and 0.2445 $\pm$ 0.0022, respectively.

Ab Initio Calculations. Quantum mechanical calculations were performed using the Gaussian 94 program.[19] This program was run on a DEC Alpha and Intel Pentium Pro 200 MHz personal computer. Molecular structures were built using Hyperchem (Hypercube, Inc.) and Chem 3D programs (Cambridgesoft, Corp.). Schematic representations of molecular orbitals were produced using Chem3D and the Molden program (Gjis Schaftenlander, The Netherlands). Schematic diagrams of molecular structures were rendered using the POV-RAY raytracing engine (POV, Inc.).

Calculations were performed at the B3LYP/D95//B3LYP/D95 level of theory. This includes electron correlation using Becke's hybrid functional[20] and Dunning's D95 basis set.[21] Orbitals were plotted using CambridgeSoft's Chem 3D 4.0. Geometry optimization was carried out with or without symmetry restrictions as applicable. The lowest energy structure was taken as the best description of the molecule of interest.

Results

Preliminary results on the regioselective chloride ion loss from polychlorodibenzo-*p*-dioxins have been reported.[12,22] The method of calculation (see Experimental Section) takes into account the natural abundance of the chlorine isotopes, and the results (Tables 1 and 2) represent total chloride ion lost from the labeled positions. The $[^{35}Cl^-]/[^{37}Cl^-]$ ion abundance ratios for certain chlorine-37 regiospecifically enriched PCDDs measured with the EM–MS instrument show that the fraction of chloride ion arising from a given position varies with electron energy (Table 1). Among this series, 1,2,3,7,8-pentachloro-, and 1,2,3,4,7,8-hexachlorodibenzo-*p*-dioxins were labeled in three different positions.[14] Because of molecular symmetry, the latter represents an example in which all possible positions could be studied.

Several aspects to these data provide confidence in the results. First, a comparison of the fraction of ^{37}Cl$^-$ measured by standard ECNI-MS on Kratos and JEOL instruments is close or very close to the fraction of ^{37}Cl$^-$ measured at 0.03 eV on the EM–MS instrument (Table 2). It is well-established that the distribution of electron energies under standard ECNI-MS conditions is at a maximum close to 0 eV.[16] Second, if the discontinuities at 0.5 eV for chlorine-7 and 1.0 eV for chlorine-1 loss (Figure 2) can be overlooked, the sum of the fractional ^{37}Cl$^-$ from the enriched postions of 1,2,3,4,7,8-hexachlorodibenzo-*p*-dioxins when doubled for symmetry total to a value close to 1.0 at three different electron energies. Finally, chloride ion ejection occurs with equal probability or very close to it from the two positions for symmetrically substituted 2(^{37}Cl),3- and 1(^{37}Cl),4-dichloro-dibenzo-*p*-dioxins at all electron energies.

The latter result has special significance since previous studies have suggested there can be chlorine isotope effects of as much as 40%[23] under mass spectrometry conditions, and even the

(14) Mahiou, B.; Deinzer, M. L. *J. Labelled Compd. Radiopharm.* **1992**, *31*, 261–287.

(15) Suntio, L. R.; Shiu, W. Y.; Mackay, D. *Chemosphere* **1988**, *17*, 1249–1290.

(16) Hites, R. A.; Ong, V. S. *Mass Spectrom. Rev.* **1994**, *13*, 259–283.

(17) Fenzlaff, H.-P.; Illenberger, E. *Int. J. Mass Spectrom. Ion Processes* **1984**, *59*, 185–202.

(18) Chang, Y.-S.; Laramée, J. A.; Deinzer, M. L. *Anal. Chem.* **1991**, *63*, 2715–2718.

(19) Frisch, M. J.; Trucks, G. W.; Schlegel, H. B.; Gill, P. M. W.; Johnson, B. G.; Wong, M. W.; Fooresman, J. B.; Robb, M. A.; Head-Gordon, M.; Replogle, E. S.; Gomperts, R.; Andres, J. L.; Raghavachari, K.; Binkley, J. S.; Gonzalez, C.; Martin, R. L.; Fox, D. J.; Defrees, D. J.; Baker, J.; Stewart, J. J. P.; Pople, J. A. Gassian 94, Gaussian, Inc.: Pittsburgh, PA, 1993.

(20) Becke, A. D. *J. Chem. Phys.* **1993**, *98*, 5648–5652.

(21) Dunning, T. H., Jr.; Hay, P. J. In *Methods of Electronic Structure Theory*; Schaefer, H. F., III, Ed.; Plenum: New York, 1977, pp 1–27.

(22) Berkout, V.D.; Laramée, J. A.; Deinzer, M. L. *Proc. 44th ASMS Conf. Mass Spectrom. Allied Topics,* Portland, OR, May 12–16, 1996.

(23) Zakett, D.; Flynn, R. G. A.; Cooks, R. G. *J. Phys. Chem.* **1978**, *82*, 2359–2362.

Table 1. Total Chloride Ion Loss (%)[a] from Labeled Positions of Regiospecifically Labeled Polychlorodibenzo-*p*-dioxins at Various Electron Energies (eV)

chlorodibenzo-*p*-dioxin	0.03	0.25	0.50	0.75	1.00	1.25	1.50	2.00
1,2(^{37}Cl)-di-	56.9 ± 1.1		60.4 ± 0.4		58.2 ± 0.8		60.2 ± 1.7	58.0 ± 3.6
1(^{37}Cl),3-di-[b]	51.1 ± 2.2		50.5 ± 1.3		48.2 ± 1.9	48.2 ± 2.0	47.7 ± 1.7	50.2 ± 2.2
1(^{37}Cl),4-di-	50.3 ± 1.1		50.4 ± 0.7		50.3 ± 1.0		49.6 ± 1.8	51.3 ± 4.3
2(^{37}Cl),3-di-	50.1 ± 1.2	51.7 ± 0.8	50.0 ± 0.8		50.4 ± 1.0		50.9 ± 1.7	48.7 ± 1.8
1(^{37}Cl),7,8-tri-	31.2 ± 1.4		31.3 ± 0.6		29.4 ± 0.7		31.6 ± 0.6	28.2 ± 1.2
2(^{37}Cl),7,8-tri-	23.7 ± 2.1		21.6 ± 2.1		21.0 ± 1.8		19.5 ± 3.0	21.2 ± 4.5
1,2,3(^{37}Cl)-tri-	41.9 ± 2.6		43.5 ± 0.5		45.8 ± 0.7		44.0 ± 1.4	50.9 ± 1.8
1(^{37}Cl),2,3,4-tetra-[c]	19.1 ± 1.3	19.3 ± 1.2	19.0 ± 1.2		19.8 ± 1.4		22.7 ±2.2	27.5 ± 1.5
1(^{37}Cl),2,3,7,8-penta-[d]	43.8 ± 1.3	43.3 ± 1.7	35.3 ± 1.6	33.8 ± 1.6	32.2 ± 3.0			
1,2(^{37}Cl),3,7,8-penta-	20.9 ± 1.8		22.2 ± 1.8		22.2 ± 2.9			
1,2,3(^{37}Cl),7,8-penta-	21.5 ± 1.6	21.9 ± 1.7	19.8 ± 1.6	24.4 ± 2.2	27.5 ± 2.4	32.9 ± 3.3		
1(^{37}Cl),2,3,4,7,8-hexa-	33.5 ± 0.8	32.7 ± 0.9	32.2 ± 0.7	30.2 ± 1.6	25.1 ± 2.2	25.9 ± 2.2		
1,2(^{37}Cl),3,4,7,8-hexa-	13.7 ± 0.8		12.8 ± 1.4		14.1 ± 1.4			
1,2,3,4,7(^{37}Cl),8-hexa-	2.2 ± 1.1	2.6 ± 1.3	5.8 ± 1.6	5.1 ± 1.6	7.6 ± 1.9	9.9 ± 1.9		

[a] The method of calculation takes into account the natural abundance of the chlorine isotopes at the unlabeled positions. [b] (^{37}Cl) ion loss at 1.75 eV is 48.6 ± 2.0%. [c] (^{37}Cl) ion loss at 1.75 eV is 24.5 ± 2.7%. [d] (^{37}Cl) ion loss at 0.38 eV is 42.1 ± 1.8%.

Table 2. Total Chloride Ion Loss (%)[a] from Labeled Positions of Regiospecifically Labeled Polychloridibenzo-*p*-dioxins under Electron Capture Negative Ion Mass Spectrometry Conditions

chlorodibenzo-*p*-dioxin	EM−MS (0.03 eV)	Kratos MS50[b]	JEOL DX-303[b]
1,2(^{37}Cl)-di-	56.9 ± 1.1	59.1 ± 0.8	54.6 ± 0.8
1(^{37}Cl),3-di-	51.1 ± 2.2	50.4 ± 0.4	51.0 ± 1.0
1(^{37}Cl),4-di-	50.3 ± 1.1	47.4 ± 0.3	47.0 ± 0.5
2(^{37}Cl),3-di-	50.1 ± 1.2	48.9 ± 0.8	47.9 ± 0.4
1(^{37}Cl),7,8-tri-	31.2 ± 1.4		29.1 ± 0.5
2(^{37}Cl),7,8-tri-	23.7 ± 2.1		19.6 ± 1.5
1,2,3(^{37}Cl)-tri-	41.9 ± 2.6	40.2 ± 0.8	44.4 ± 1.5
1(^{37}Cl),2,3,4,-tetra-	19.1 ± 1.3	17.8 ± 0.6	25.7 ± 1.3
1(^{37}Cl),2,3,7,8-penta-	43.8 ± 1.3	41.6 ± 0.4	
1,2(^{37}Cl),3,7,8-penta-	20.9 ± 1.8	21.8 ± 0.4	
1,2,3(^{37}Cl),7,8-penta-	21.5 ± 1.6	19.2 ± 0.5	
1(^{37}Cl),2,3,4,7,8-hexa-	33.5 ± 0.8	33.2 ± 0.6	
1,2(^{37}Cl),3,4,7,8-hexa-	13.7 ± 0.8	14.3 ± 1.0	
1,2,3,4,7(^{37}Cl),8-hexa-	2.2 ± 1.1	2.5 ± 0.3	

[a] The calculations for chloride ion loss take into account the natural abundance of both chlorine isotopes. [b] Methane used as reagent gas at 0.6 Torr.

present data (Table 2) indicate a discrimination against the loss of ^{37}Cl$^-$ that is outside experimental error when analyzed by standard ECNI-MS methods. In fact in 14 out of 20 measurements made by standard ECNI-MS on sector instruments, chloride ion loss from the labeled position is lower than that produced by the EM−MS system, and of the six that are higher, only three, 1,2(^{37}Cl)-dichlorodibenzo-*p*-dioxin on the Kratos instrument and 1,2,3(^{37}Cl)-tri- and 1(^{37}Cl),2,3,4-tetrachlorodibenzo-*p*-dioxin on the JEOL instrument, are outside the range of experimental error. The lower ^{37}Cl$^-$ yield may be due in part to the difference in diffusion coefficients of the chlorine isotopes. Typical ion source conditions in standard ECNI-MS experiments are an electric field intensity $E \approx 2$ V/cm, and a pressure $p \approx 0.5$ Torr.[24] The parameter $E/p \approx 2$ V/cm·Torr which means that the motion of the ion in the source can be described by a "low-field" approximation.[25] As a result, ions drift with a steady-state velocity, v_d, that is achieved through a balance between ion acceleration in the ion field direction and deceleration by collisions with reagent gas molecules:

$$v_d = KE \qquad (1)$$

Since the mobility coefficients, K, are directly proportional to the diffusion coefficients of the ions, the heavier ^{37}Cl$^-$ moves more slowly and remains in the ion source 1.0−1.5% longer than ^{35}Cl$^-$ which provides a greater opportunity for the heavier ions to undergo ion−ion or ion−molecule reactions with neutrals or with charged species generated from the reagent gas. Although other explanations are possible, it is clear from the data (Table 2) that chlorine isotope effects are not important.

The electron energy, ϵ_{max}, required to record the maximum molecular radical anion intensity, does not vary much with the degree of chlorination of the PCDDs. Five congeners ranging from trichloro- to hexachlorodioxins show negative ion resonances, i.e., ϵ_{max} values, within the narrow electron energy range 0.09 eV (Table 3). Lower chlorinated dioxins yield no apparent molecular ions which is consistent with the known behavior of these compounds when analyzed under standard ECNI-MS conditions.[26]

When the electron energy is scanned over the range 0−10 eV with the mass set to record the molecular ions, a maximum is observed near 0 eV. Similarly when the mass is set to record ^{35}Cl$^-$ abundances, maxima around 0 and 4 eV (Figure 1) are clearly observed for all dioxins. The low energy resonances for the ^{35}Cl$^-$ appear at electron energies slightly higher than the corresponding ones for the formation of the molecular ions. Most of these low energy peaks are non-Gaussian, and some of them show evidence that they consist of at least two peaks. Deconvolution of the major peaks ~0 eV for 1,2,3,4-tetra-, and 1,2,3,7,8,-pentachlorodibenzo-*p*-dioxins with a nonlinear curve-fitting algorithm (Figure 1) indicates there is at least another negative ion state located around 1 eV for these PCDDs. The deconvoluted data for all PCDDs indicate that ϵ_{max} values for the first negative ion states are associated with slightly lower electron energies (Table 3) than would otherwise be indicated by the nondeconvoluted scans. The ϵ_{max} values obtained from deconvolution decrease with the degree of chlorination which is consistent with a lowering of the orbital energies as the number of chlorines on the molecules increase.[26]

A general conclusion that can be drawn from the chloride ion yield data (Table 1) is that the more highly substituted ring of the ionized dioxin molecule is the one more likely to lose the chloride ion. In 2(^{37}Cl)7,8- and 1(^{37}Cl)7,8-trichlorodioxins, for example, 77 and 69%, respectively, of the chlorines are lost from positions 7 or 8 with electrons of lowest energies.

(24) Stemmler, E. A.; Hites, R. A. *Biomed. Environ. Mass Spectrom.* **1988**, *15*, 659−667.

(25) Mason, E. A.; McDaniel. E. W. *Transport Properties of Ions in Gases*, Wiley: New York, 1988.

(26) Laramée, J. A.; Arbogast, B. C.; Deinzer, M. L. *Anal. Chem.* **1988**, *60*, 1937−1943.

Table 3. Electron Attachment Energies (ϵ_{max}) (eV) for the Formation of Molecular (M⁻•) and Chloride (Cl⁻) Ions from Polychlorodibenzo-*p*-dioxins

chlorodibenzo-*p*-dioxin	M⁻•(expt)	M⁻•(calcd)ᵃ	Cl⁻ᵇ	Cl⁻ᶜ (expt)	Cl⁻ (calcd)ᵃ	Δ|ε|ᵉ
1,2(³⁷Cl),3,4,7,8-hexa-	0.12 ± 0.06	−0.14	0.22 ± 0.02			
1,2,3,4,7,8-hexa-				0.23//1.2//3.83ᵈ	0.09//0.86//3.66	0.14//0.34//0.17
1,2,3,7,8-penta-	0.20 ± 0.06	0.01	0.33 ± 0.05	0.18//0.94//3.83	0.21//0.98//3.78	0.03//0.04//0.05
1,2,4,7,8-penta-	0.16 ± 0.05	−0.04	0.27 ± 0.03	0.16//0.98//3.83	0.25//0.97//3.76	0.09//0.01/0.07
1(³⁷Cl),2,3,4-tetra-	0.11 ± 0.05	0.20	0.41 ± 0.03	0.40//1.06//3.98⁽ᵈ⁾	0.33//1.26//3.99	0.07//0.24//0.01
1,2,3(³⁷Cl)-tri-	0.16	0.36	0.45 ± 0.04	0.38//1.08//4.22	0.46/0.82//4.13	0.08//0.26//0.09
1(³⁷Cl),7,8-tri-			0.47	0.36//1.06//4.23	0.33//1.29//4.10	0.03//0.23//0.13
2(³⁷Cl),7,8-tri-			0.52	0.40//1.28//4.05	0.31//1.28//4.07	0.09//0.00//0.02
2(³⁷Cl)3-di-			0.55 ± 0.03	0.45//1.21//4.08	0.54//1.58//4.31	0.09//0.37//0.23

ᵃ $\hat{\epsilon} = (x + 1.874)/1.147$. (See Discussion). Orbital energies, x, calculated by B3LYP/95//B3LYP/D95 method. ᵇ First experimental Cl⁻ resonance peaks before deconvolution. ᶜ First Cl⁻ resonance peaks deconvoluted with a nonlinear curve-fitting algorithm. ᵈ Data obtained at 190−200 °C ion source temperature. ᵉ Absolute difference between calculated and experimental ϵ_{max} values for chloride ion dissociative resonance.
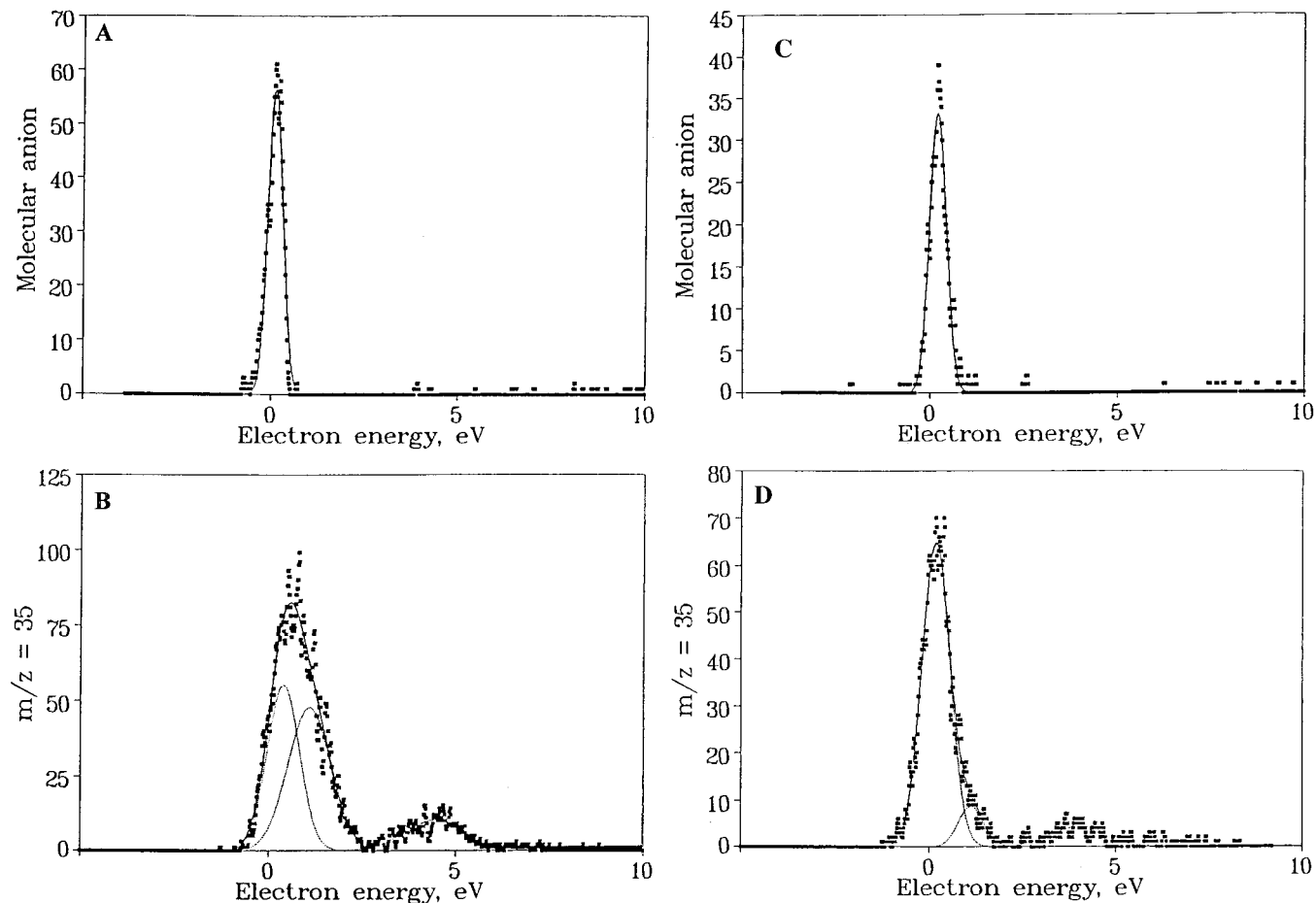
Figure 1. Electron energy scans for (A) molecular ion and (B) ³⁵Cl⁻ ion loss from 1,2,3,4-tetrachlorodibenzo-*p*-dioxin and (C) molecular ion and (D) ³⁵Cl⁻¹ ion loss from 1,2,3,7,8-pentachlorodibenzo-*p*-dioxin under electron capture negative ion conditions using the electron monochromator−mass spectrometer.

This pattern is also observed for pentachloro- and hexachloro-dioxins which loose 86 and 94% of the chlorines respectively from the more highly substituted ring at 0.03 eV electron energy. In each of these examples the chloride ion is most likely to come from the more substituted ring even at higher ionizing electron energies. The higher rates of chloride ion loss from the more substituted ring can be rationalized on the basis of classical steric relief or stabilization of the radical by the electron-withdrawing chlorines.

Regioselective loss of chloride ions from ionized dioxins generally appear to be dependent on the energies of the ionizing electrons. Chlorines at the 2-position, however, are somewhat less sensitive to the electron energies at least within the limits 0−1 eV. This pattern is observed for 2(³⁷Cl),7,8-trichloro-dibenzo-*p*-dioxin and for 1,2(³⁷Cl)-dichlorodibenzo-*p*-dioxin

over a 2 eV electron energy range. The effect is particularly striking for 1,2,3,7,8-pentachloro- and 1,2,3,4,7,8-hexachloro-dioxins, where losses at other positions in comparison are much more sensitive to the ionizing electron energies. Chlorine loss from the 2-position in these compounds may be more important with electrons of energies greater than 1 eV. This is suggested by the results for 1(³⁷Cl),2,3,4-tetrachlorodibenzo-*p*-dioxin where chlorines in the 2-position show greater sensitivity to the energy of the ionizing electron in the range 1−2 eV. In this example about 40% of the chloride ion comes from the 1-(+4)-position at 1.0 eV and rises to about 55% at 2 eV. By difference chloride ions from the 2-(+3)-positions must decrease by 15% over this energy range.

Because different positions were labeled in several penta-chloro- and hexachlorodioxins, these congeners provide the

better models for analyzing the effects of electron energy on the regiochemistry of chloride ion loss. The percentage of chloride ion arising from position-1 in both 1,2,3,7,8-penta-chloro- and 1,2,3,4,7,8-hexachlorodioxins decreases significantly between 0.03 and 1.0 eV while loss of chlorine-3 from pentachlorodioxin and chlorine-7 from hexachlorodioxin increase over this range. Chloride ions clearly come from all positions of the PCDDs, but the fractional amounts that arise from these positions vary with the electron energies.

Unfortunately, it was not possible to acquire accurate $[^{35}Cl^-]/$ $[^{37}Cl^-]$ ratio information at electron energies greater than 2 eV because of the low ion intensities at these energies. The negative ion state which appears at $\sim$4 eV (Figure 1) is only $^1/_{10}$–$^1/_{20}$ the intensity of the peak near 0 eV. However, the trends suggest that while chloride ions arise mostly from the 1-position in pentachloro- and hexachlorodioxins at low electron energies (Figure 2), a greater fraction arises from position-7 in hexachlorodioxin at the higher electron energy, i.e., $\epsilon_{max} = 3.8$ eV. Pentachlorodioxin shows a rise in the chloride ion lost at position-3 as the electron energy is increased from 0 to 1 eV, but the total fraction of chlorine accounted for decreases from 0.86 to 0.74 over this energy range. An increased fraction of the chloride ion must, therefore, come from positions 7 and 8 at 1 eV, and this trend may continue so that a significant fraction of chloride ion arises from these positions at 3.8 eV.
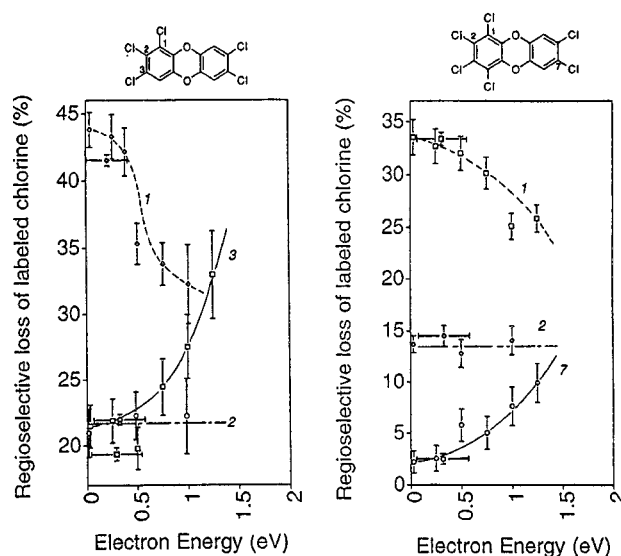
Discussion

There are two important processes for production of ions in ECNI-MS. These are resonance electron capture that produces detectable molecular ions and dissociative electron capture which results in fragment ions.[1] In the simplest interpretation these processes can be viewed as the capture of an electron by the neutral molecule in its electronic ground state which gives rise via a Franck–Condon transition to a radical anion in a higher electronic state. If one accepts this simple vertical transition, a direct comparison of the electron attachment energies between the two processes can be made. In one process, i.e., resonance capture, stabilization of the radical anion (eq 1) takes place by some mechanism—in ECNI-MS the buffer gas helps to remove excess energy—and the ion is sufficiently long-lived ($\geq 10^{-6}$ s) to be detected. In dissociative electron capture (eq 2)

$$RX + e^- \rightarrow RX^{-\bullet} \qquad (1)$$

$$RX + e^- \rightarrow [RX^{-\bullet}] \rightarrow R^\bullet + X^- \qquad (2)$$
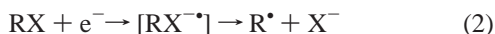
the radical anion has a very short (10^{-13}–10^{-15} s) lifetime, and only fragment ions are detected from this transient negative ion. The process involved is referred to as a shape resonance and arises from an attractive potential due to the electron–dipole interaction, and a repulsive potential from the angular momentum of the electron associated with a given orbital.[8] The opposing potentials create a shallow potential well on the continuum where the electron is temporarily trapped, hence the designation temporary negative ion.

A number of studies have been reported showing linear relationships between calculated virtual orbital energies using Koopmans' theorem and the experimental resonance electron attachment energies[11,27] or electron affinities[28] of organic

(27) Howard, A. E.; Staley, S. W. In *Resonances*; Truhlar, D. G., Ed.; American Chemical Society: Washington, DC, 1984. pp 183–192.

(28) Heinrich, N.; Koch, W.; Frenking, G. *Chem. Phys. Lett.* **1986**, *124*, (1), 20–25.

Figure 2. Electron energy-dependent regioselective loss of chloride ion from labeled positions in 1,2,3,7,8-pentachloro- and 1,2,3,4,7,8-hexachlorodibenzo-*p*-dioxins. Data obtained with the EM–MS instrument. Short horizontal lines indicate relative ion loss under standard ECNI-MS conditions measured on a sector instrument.

Table 4. Experimental and Calculated Attachment Energies for Aromatic Compounds

compd	AE (eV) expt[a]	AE (eV) calcd[b]	molecular orbital E (eV)
benzonitrile	0.58	0.14	−1.708
	2.5	2.07	0.501
benzene	1.07	1.42	−0.244
	4.88	4.93	3.784
	8.85	8.89	8.316
chlorobenzene	0.825	1.00	−0.727
	1.74	2.07	0.494
	4.59	4.60	3.396
	8.22	8.43	7.790
phenol	0.883	1.30	−0.385
	1.69	1.63	0.001
	4.85	4.59	3.386
styrene	0.25	0.64	−1.145
	1.05	1.39	−0.282
	2.48	2.72	1.246
	4.67	4.72	3.538
toluene	1.19	1.47	−0.191
	4.89	4.93	3.782
	8.37	8.31	7.658

[a] Electron transmission data for AE (eV) expt from Christophorou, L. G.[8] p 464. [b] Values calculated using the scaling equation, eq 3.

molecules. Thus, Staley and Strnad,[29] recently reported finding strong correlations between the experimental electron attachment energies obtained from electron transmission spectroscopic data for a large number of aromatic and unsaturated hydrocarbons, with their π virtual orbital energies calculated by several Gaussian basis sets. A similar approach was used in the present study. The experimental electron attachment energies obtained from the literature[8] for some substituted benzenes (Table 4) and the vertical attachment energies for the polychlorodibenzo-*p*-dioxins (Table 5) were correlated with the π virtual orbital energies obtained from calculations performed at the B3LYP/D95//B3LYP/D95 level of theory. Geometry optimizations were performed on the neutral ground states, thereby allowing a comparison of the orbital energies associated with both molecular and fragment ion production. If only π orbitals are

(29) Staley, S. W.; Strnad, J. T. *J. Phys. Chem.* **1994**, *98*, 116–121.

Table 5. Experimental and Calculated Attachment Energies for Polychlorodibenzo-*p*-dioxins

compd	AE (eV) expt	AE (eV) calcd[a]	molecular orbital E (eV)
1,2,3,4,7,8-HCDD	0.12[b]	−0.14	−2.031
	0.23	0.09	−1.775
	1.21	0.86	−0.888
	3.83	3.66	2.324
1,2,3,7,8-PCDD	0.2[b]	0.01	−1.862
	0.18	0.21	−1.630
	0.94	0.98	−0.753
	3.84	3.78	2.460
1,2,3,4-TCDD	0.11[b]	0.20	−1.65
	0.4	0.33	−1.49
	1.06	1.26	−0.429
	3.98	3.99	2.702
1,2,3-TCDD	0.16[b]	0.36	−1.464
	0.38	0.46	−1.351
	1.08	0.82	−0.938
	4.22	4.13	2.856
1,2,4,7,8-PCDD	0.16[b]	−0.04	−1.920
	0.16	0.25	−1.589
	0.98	0.97	−0.760
	3.83	3.76	2.437
1,7,8-TCDD	0.36	0.33	−1.497
	1.06	1.29	−0.390
	4.23	4.10	2.832
2,7,8-TCDD	0.4	0.31	−1.513
	1.28	1.28	−0.408
	4.05	4.07	2.794
2,3-DCDD	0.45	0.54	−1.256
	1.21	1.58	−0.060
	4.08	4.31	3.065

[a] Values calculated using the scaling equation, eq 3. [b] Molecular ion resonance. All other resonances in this column are for the chloride ion.
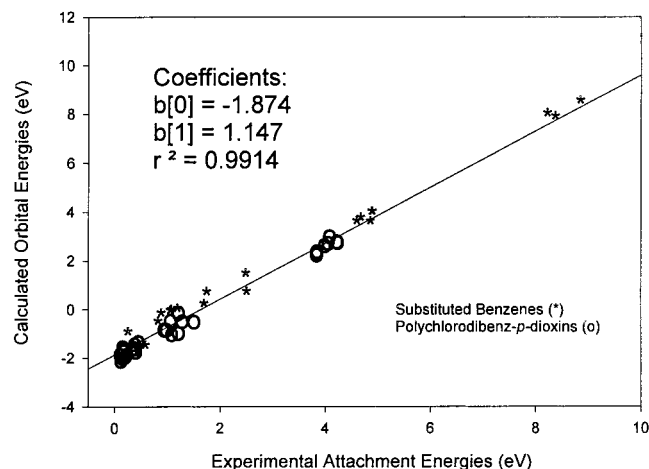
Figure 3. Calculated orbital energies vs experimental attachment energies for aromatic compounds.

considered for both substituted benzenes and PCDDs, an excellent correlation is observed (Figure 3) between the experimental electron attachment energies (ϵ_{max}) and the virtual orbital energies. From the regression line (eq 3)

$$\hat{\epsilon} = (x + 1.874)/1.147 \qquad (3)$$

where x is the calculated orbital energy the predicted electron energies can be obtained (Table 3). The differences between the experimental and calculated values (Table 3) are generally within the experimental error (0.2 eV) of the measurement.

The calculations for PCDDs show five unoccupied low-lying π orbitals (Figures 4−6). Four of these orbitals can be associated with the experimental attachment energies through the scaling relationship, one for production of the molecular ion and three for the chloride ions. The molecular ions recorded for five dioxins (Table 3) are associated with LUMOs, and the first negative ion state producing chloride ion from each PCDD is predicted to involve the LUMO + 1 (Figures 4−6). The remaining resonances are associated with higher π^* orbitals. Thus, 1,2,3,7,8-pentachlorodibenzo-*p*-dioxin has experimental resonance peaks at 0.94 and 3.83 eV (Table 3) which correspond to virtual orbital energies −0.75 eV (LUMO + 5) and 2.46 eV (LUMO + 10) (Table 5, Figure 4), respectively. It is important to note that LUMO + 6 through LUMO + 9 as well as LUMO + 11 (data not shown) for this compound are σ orbitals. Only LUMO + 10 in the higher energy region is a π orbital. A similar pattern is found for the other PCDDs, although different orbitals may be associated with the higher energy resonances.

For each PCDD there is one remaining low lying π^* orbital available, i.e., the LUMO + 3 (Figures 4−6) that did not correlate with an experimental negative ion resonance. Using the scaling relationship (eq 3), the electron attachment energies associated with this orbital would be 0.27 eV for 1,2,3,7,8-pentachloro-, 0.20 eV for 1,2,3,4,7,8-hexachloro-, and 0.74 eV for 1,2,3,4-tetrachlorodibenzo-*p*-dioxin (Figures 4−6). It is possible that the first experimental peak in the electron energy scans of the chloride ion from each PCDD may be a composite of three, not two, peaks. Deconvolution into three peaks, however, did not give as good a correlation with the caculated orbital energies.

It was recognized early on that dissociative electron capture involving π^* orbitals must involve a mechanism for $\pi^*-\sigma^*$ mixing. Through-space symmetry-allowed interactions between π^* and σ^* orbitals are strongly supported by experimental evidence in dissociative attachment studies of chloronorbornyl[30] and other chlorinated multicyclic ring[31] systems. In the case of planar molecules in which the chlorine is attached directly to the C=C system as in vinyl choride and chlorobenzenes, out-of-plane distortions of the C−Cl bond in the transition state[32] or a "bent bond" transition-state model[33] have been proposed. Using ab initio calculations, Allan and co-workers[34] have demonstrated strong $\pi^*-\sigma^*$ mixing as the C−Cl bond stretches in the process of producing benzylic halide ions from halobenzyl halides at low electron energies. The phenylic halide ions are also produced at low energies from π^* states, but with much lower yields. Predissociation via out-of-plane bending was used to rationalize these results.

In contrast to dissociative attachment involving C−Cl σ^* orbitals, electrons in π^* orbitals experience higher angular momentum barriers toward tunneling, and the transient negative ions, therefore, have much longer lifetimes.[11,35] Coupling between the π^* and σ^* orbitals is more likely which in turn increases the dissociative attachment cross section.[11,35] When π orbitals are available, they can become involved in the dissociative process, and where direct attachment of the electron into an unoccupied σ orbital takes place, the resonances are generally found at higher energies.[35]

(30) Pearl, D. M.; Burrow, P. D.; Nash, J. J.; Morrison, H.; Jordan, K. D. *J. Am. Chem. Soc.* **1993**, *115*, 9876−9877.

(31) Pearl, D. M.; Burrow, P. D.; Nash, J. J.; Morrison, H.; Nachtigallova, D.; Jordan, K. D. *J. Phys. Chem.* **1995**, *99*, 12379−12381.

(32) Stricklett, K. L.; Chu, S. C.; Burrow, P. D. *Chem. Phys. Lett.* **1986**, *131*(3), 279−283.

(33) Freeman, P. K.; Srinivasa, R.; Campbell, J.-A.; Deinzer, M. L. *J. Am. Chem. Soc.* **1986**, *108*, 5531−5536.

(34) Bulliard, C.; Allan, M.; Haselbach, E. *J. Phys. Chem.* **1994,** *98*, 11040−11045.

(35) Jordan, K. D.; Burrow, P. D. In *Resonances*; Truhlar, D. G., Ed.; American Chemical Society: Washington, DC, 1984; pp 165−182.
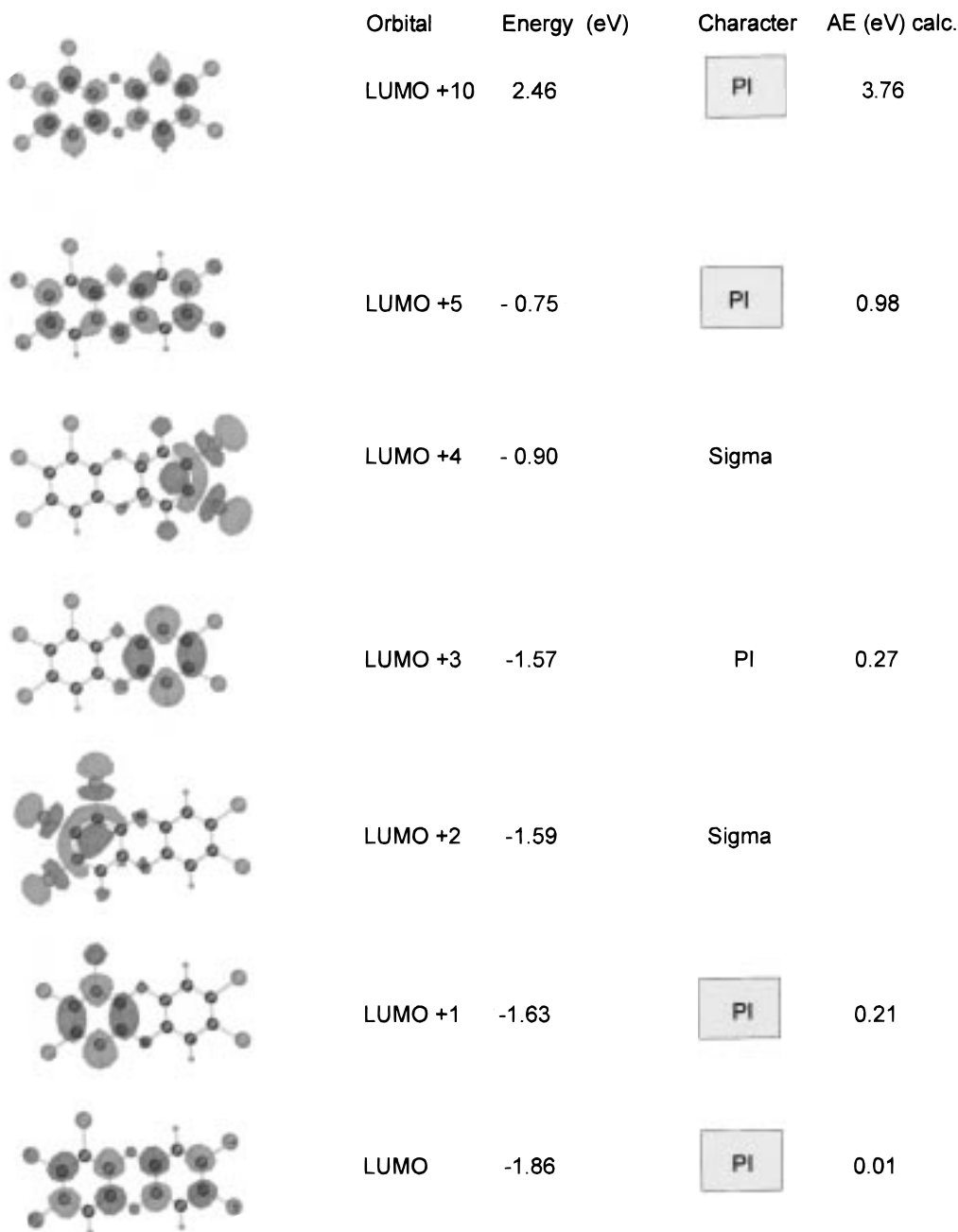
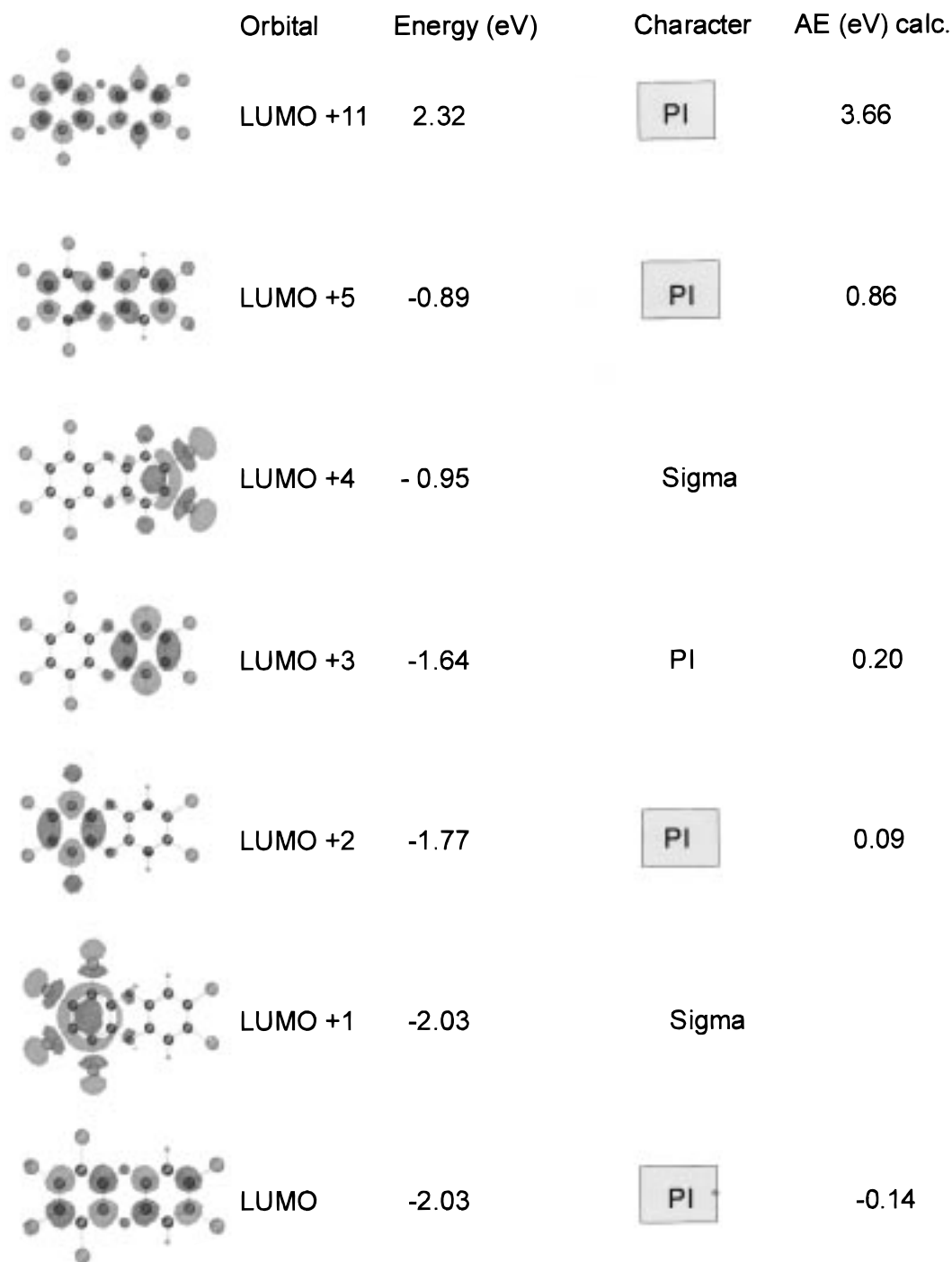| Orbital	Energy (eV)	Character	AE (eV) calc.
LUMO +10	2.46	PI	3.76
LUMO +5	- 0.75	PI	0.98
LUMO +4	- 0.90	Sigma	
LUMO +3	-1.57	PI	0.27
LUMO +2	-1.59	Sigma	
LUMO +1	-1.63	PI	0.21
LUMO	-1.86	PI	0.01

Figure 4. Virtual orbitals and energies (eV) of 1,2,3,7,8-pentachlorodioxin represented as isosurfaces with a contour value of 0.03 hartree. Boxes represent orbitals that correlate with experimental vertical attachment energies.

In the present studies, the excellent correlation between π virtual orbital energies and experimental attachment energies (Figure 3) as well as the low-energy electrons needed to produce chloride ions argues for π^*-state initiation of the dissociative process. The relevant π^* states are close in energy to nearby σ^* states, permitting mixing of these orbitals as the carbon−chlorine bond bends out of the plane of the aromatic ring. Close inspection of the virtual orbital energies for 1,2,3,7,8-penta-chlorodibenzo-p-dioxin (Figure 4), for example, shows that the LUMO + 2 σ orbital, is only 0.04 eV higher in energy than the LUMO + 1 and the LUMO + 5 orbital, which corresponds to the experimental attachment energy 0.97 eV, is just 0.15 eV below the LUMO + 4. In all of the PCDDs studied, the difference in energies between the virtual π orbitals associated with the first two experimental resonances and the nearest σ orbitals were never greater than 0.5 eV. These are not small differences, but a change in energy of this magnitude for the

potential curve representing increasing C−Cl bond distances as the system progresses from π^* to σ^* is not unreasonable. Calculations by the AM1 unrestricted Hartree−Fock method for 3,6-dichlorodibenzofuran showed a progression from π^* to σ^* as the C−Cl bond distance increased with a final energy difference of 40 kcal/mol.[36]

The dissociative attachment resonance at ∼3.8 eV was initially assumed to involve a σ^* orbital. However, the calculated orbital energies that fit the correlation best (Figure 3) are all π^*, and for 1,2,3,7,8-pentachlorodioxin the energy is 1.36 eV above the nearest virtual σ orbital. The higher energy resonances for the PCDDs generally correlate with π^* orbitals that are >1 eV from the nearest σ orbital.. Allan and co-workers [34] observed a resonance at 4.5 eV in their studies on halobenzyl halides

(36) Chang, Y.-S. Ph. D. Thesis, "The Synthesis and Electron Capture Negative Ion Mass Spectrometry of Polychlorinated Diphenyl Ethers and Dibenzofurans," 1990, Oregon State University, pp 132−154.

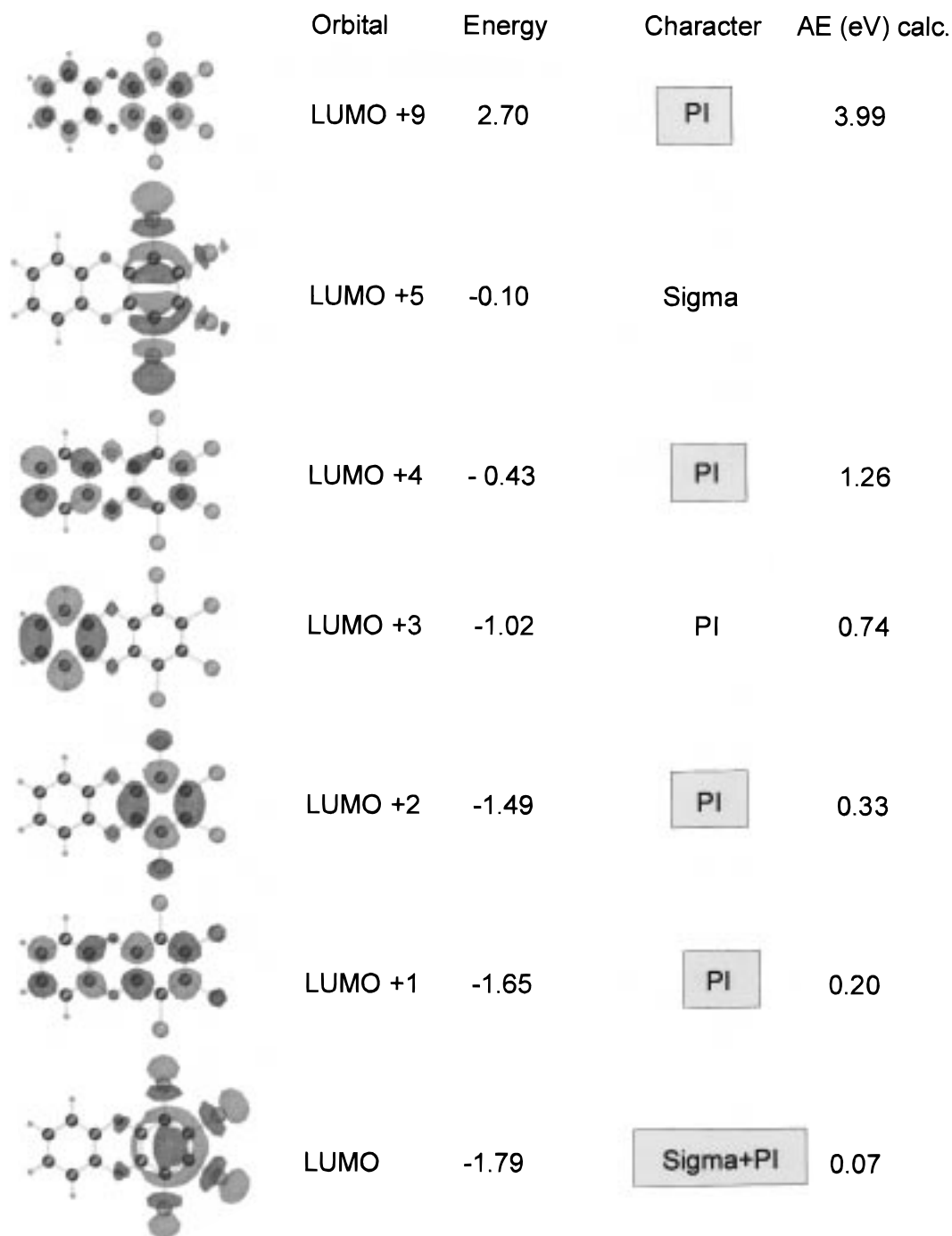|	Orbital	Energy (eV)	Character	AE (eV) calc.
	LUMO +11	2.32	PI	3.66
	LUMO +5	-0.89	PI	0.86
	LUMO +4	- 0.95	Sigma	
	LUMO +3	-1.64	PI	0.20
	LUMO +2	-1.77	PI	0.09
	LUMO +1	-2.03	Sigma	
	LUMO	-2.03	PI	-0.14

Figure 5. Virtual orbitals and energies (eV) of 1,2,3,4,7,8-hexachlorodioxin represented as isosurfaces with a contour value of 0.03 hartree. Boxes represent orbitals that correlate with experimental vertical attachment energies.

from which the phenylic halide was lost. A (π, π*s) state was proposed for this resonance in which the extra electron is captured in a very diffuse totally symmetrical s orbital of the parent singlet excited state (π, π*). The total wave function of this state is symmetrical with respect to the benzene ring and a transition to the σ* orbital is symmetry-allowed, thereby allowing facile phenylic carbon−chlorine bond cleavage. A similar mechanism may apply to the PCDDs. The excellent correlation (Figure 3) between the experimental attachment energies and the calculated π* orbital energies lends strong support to this mechanism.

The orbital densities of both the LUMO + 1 and LUMO + 2 (Figure 4) is concentrated on the ring from which the chloride ion arises, and in the next higher orbitals, LUMO + 4 and

LUMO + 5, the density is shifted toward the ring containing chlorines 7 and 8, consistent with the greater chloride ion loss from these positions. A similar pattern is observed for 1,2,3,4,7,8-hexachlorodibenzo-*p*-dioxin (Figure 5). A particularly interesting result is observed for 1,2,3,4-tetrachlorodibenzo-*p*-dioxin (Figure 6) where the orbital concentration shifts from all carbon−chlorine bonds in the LUMO to carbon−chlorine bonds 1 and 4 in the LUMO + 5. The shift in the orbital density to the 1 and 4 carbons may account for the greater loss of chloride ion from these positions as the electron energy is increased (Table 1), a result that at first was perplexing, since the electron energy scan pattern was just the reverse of that observed for 1,2,3,4,7,8-hexachlorodibenzo-*p*-dioxin at low electron energies (Figure 2). Investigations on the possible relationship between orbital

Orbital	Energy	Character	AE (eV) calc.
LUMO +9	2.70	PI	3.99
LUMO +5	-0.10	Sigma	
LUMO +4	- 0.43	PI	1.26
LUMO +3	-1.02	PI	0.74
LUMO +2	-1.49	PI	0.33
LUMO +1	-1.65	PI	0.20
LUMO	-1.79	Sigma+PI	0.07

Figure 6. Virtual orbitals and energies (eV) of 1,2,3,4-tetrachlorodioxin represented as isosurfaces with a contour value of 0.03 hartree. Boxes represent orbitals that correlate with experimental vertical attachment energies.

densities and regiochemistry of dissociative chloride ion loss would benefit from transition-state model calculations on the radical anions.

Conclusions

ECNI-MS is viewed as involving two general processes, resonance electron capture (eq 1) that gives rise to the molecular ions and dissociative electron capture that yields fragment ions and radical species (eq 2). The temporary radical anion states from which these products result are classified as shape resonances or core-excited resonances.[8,35] In the former an electron attaches to an unoccupied orbital of the molecule in its ground state, while in the latter electron attachment is accompanied by promotion of the molecule to an electronically

excited state. Nuclear excited Feshbach resonances are temporary negative ion states that fall energetically below the parent state. For many polyatomic molecules Feshbach resonances give rise to long-lived ($\geq 10^{-6}$ s) molecular ions.[8] The ions produced from PCDDs involve all of these processes.

The molecular radical anions of PCDDs involve π* LUMO orbitals. Resonances for dissociative electron attachment producing chloride ions involve higher energy π* orbitals, with coupling to nearby σ* orbitals. Deconvolution of the broad negative ion resonance peak producing chloride ions near 0 eV (Figure 1a, b) using a nonlinear algorithm, indicates there are at least two temporary negative ion states, and these can be correlated nicely with the neutral molecules' π virtual orbital energies.

The bent bond transition-state[33] model or out-of-plane distortions[11,32] provides a framework for $\pi^*-\sigma^*$ orbital mixing necessary for carbon−chlorine bond dissociation. It would be enlightening to carry out ab initio calculations on the transition states to gain an understanding of the geometries involved during carbon−chlorine bond cleavage as well as to gain a better insight into the effects of electron energies on the regiochemistry of fragmentation.